



Exploring the mesoscale connectivity of phytoplankton periodic assemblages' succession in northern Adriatic pelagic habitats

Ivano Vascotto^{a,b,*}, Fabrizio Bernardi Aubry^c, Mauro Bastianini^c, Patricija Mozetič^b, Stefania Finotto^c, Janja Francé^b

^a Jozef Stefan International Postgraduate School, Jamova cesta 39, 1000 Ljubljana, Slovenia

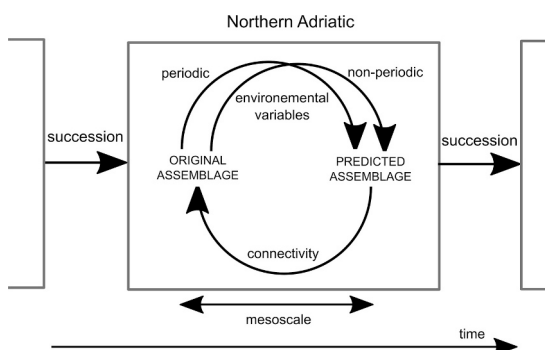
^b National Institute of Biology, Marine Biology Station Piran, Fornače 41, 6330 Piran, Slovenia

^c National Research Council—Institute of Marine Sciences (CNR—ISMAR), Arsenale Tesa 104, Castello 2737/F, 30122 Venice, Italy

HIGHLIGHTS

- The response of marine phytoplankton to temporal changes in the environment was analysed.
- Assemblages were a working model for describing the relationship between the environment and phytoplankton.
- Periodicity explained a between 39 and 46 % of the variance in environmental parameters.
- We predicted phytoplankton assemblages with more significant IndVal values using environmental periodic components.
- The northern Adriatic Sea is a connected mesoscale habitat for the phytoplankton community during autumn and winter.

GRAPHICAL ABSTRACT



ARTICLE INFO

Editor: Julian Blasco

Keywords:

Phytoplankton
Assemblages
Northern Adriatic
Phenology

ABSTRACT

An appropriate model for phytoplankton distribution patterns is critical for understanding biogeochemical cycles and trophic interactions in the oceans and seas. Because phytoplankton dynamics in coastal waters are more complex due to shallow depth and proximity to land, more accurate models applied to the correct spatial and temporal scales are needed. Our study investigates the role of the atmosphere and hydrosphere in pelagic habitat by modelling phytoplankton assemblages at two Long Term Ecological Research sites in the northern Adriatic Sea using niche-forming environmental variables (wind, temperature, salinity, river discharge, rain, and water column stratification). To study the synchronization between the phytoplankton community and these environmental variables at the two LTER sites, we applied current linear and nonlinear numerical methods for ecological modelling. The aim was to use periodic and/or non-periodic properties of the environmental variables to classify the phytoplankton assemblages at one LTER site (Gulf of Trieste - Slovenia) and then predict them at another LTER site 100 km away (Gulf of Venice - Italy). We found that periodicity played a role in the explanatory and predictive power of the environmental variables and that it was more important than non-periodic events in defining the common structure of the two pelagic habitats. The non-linear classification functions of the neural networks further increased the predictive power of these variables. We observed partial synchronization of communities at the mesoscale and differences between the original and predicted assemblages under similar

* Corresponding author at: Jozef Stefan International Postgraduate School, Jamova cesta 39, 1000 Ljubljana, Slovenia.

E-mail address: ivano.vascotto@nib.si (I. Vascotto).

<https://doi.org/10.1016/j.scitotenv.2023.169814>

Received 11 May 2023; Received in revised form 22 December 2023; Accepted 29 December 2023

Available online 4 January 2024

0048-9697/© 2024 The Authors. Published by Elsevier B.V. This is an open access article under the CC BY license (<http://creativecommons.org/licenses/by/4.0/>).

environmental conditions. We conclude that mesoscale connectivity plays an important role in phytoplankton communities in the northern Adriatic. However, the loss of periodicity of niche-forming variables due to more frequent extreme meteorological and hydrological events could loosen these connections and affect the temporal succession of phytoplankton assemblages.

1. Introduction

Historically, ecology has addressed the causes of local population patterns, while biogeography has addressed large-scale patterns in the distribution of populations and the diversity of natural systems (Ricklefs and Jenkins, 2011). A theme common to both disciplines is the definition of temporal and spatial scales, from individual organisms and their

lifespan activities (local scale) to population distributions (mesoscale and beyond). Ecological studies, in particular, typically address time spans ranging from generation times to longer population cycles (Jenkins and Ricklefs, 2011). The intermediate scales for temporal and spatial dimensions on which ecology and biogeography converge are considered relevant to population dynamics (Jenkins and Ricklefs, 2011). In the specific case of phytoplankton biogeography, it has been

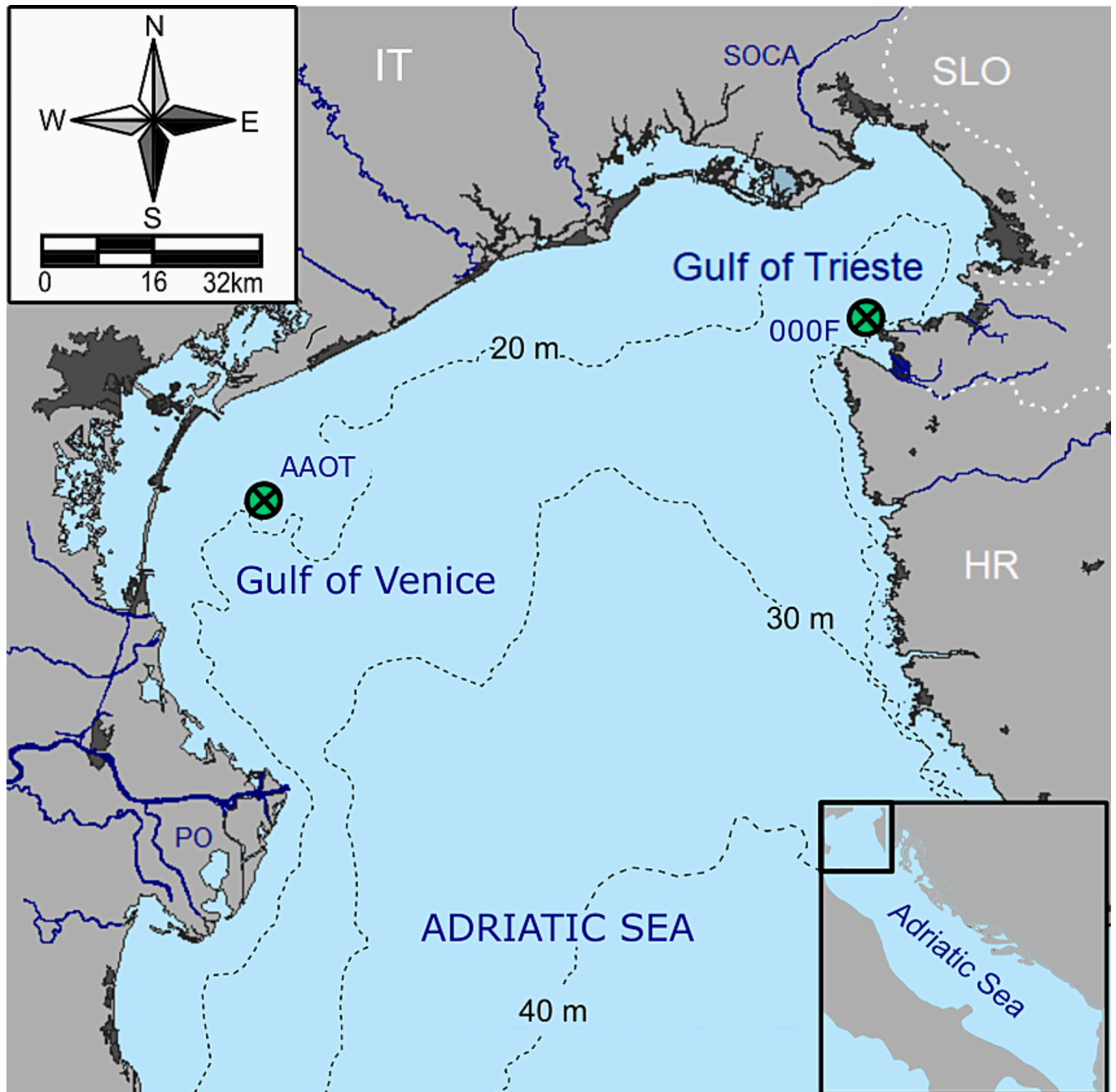


Fig. 1. Map of the study area. Both sampling stations, 000F and AAOT, represent respective LTER sites, i.e., Gulf of Trieste - Slovenia and Gulf of Venice - Italy (IT12-001-M DEIMS).

shown that the distribution of this biological compartment is generally patchy and that the current inability of climate prediction models to resolve ecosystems at the mesoscale (1–500 km) is a major obstacle to understanding the marine ecosystem as a whole (Martin, 2003). Indeed, an appropriate model for phytoplankton distribution patterns is critical for understanding trophic interactions in the ocean, biogeochemical cycles, and more generally the ecology of the marine environment (Ptacnik et al., 2008; Vallina et al., 2014).

Environmental factors and top-down control by grazers shape phytoplankton dynamics, which experience greater complexity in coastal waters due to shallow water depth and proximity to land (Salgado-Hernanz et al., 2019). The intertwined relationship between space, time, environment, and phytoplankton suggests that it would be highly interesting to study variation in all these dimensions simultaneously to partition the known variation in community composition into proportions explained by factors related to dispersal, community succession, and environmental influences (Soininen, 2010). In general, the spectrum of dynamics of ecological systems is broad, encompassing all stages between regular cycles and chaotic oscillations (May, 1976; Stone, 1993). Platt and Denmann used spectral analysis to show that marine phytoplankton are distributed in space according to the Kolmogorov 5/3 dissipation rule (Platt and Denmann, 1975) while, temporally, patterns for phytoplankton range from stable annual variations in certain biomes to the absence of a repeating pattern in others (Cloern and Jassby, 2010).

Early attempts to link phytoplankton phenology and periodicity of environmental variables were made in the 1970s when Margalef introduced the concept of phytoplankton succession, the so-called mandala, in which the main stages of succession are determined by turbulence and nutrient availability (Margalef, 1978). Based on his work, Reynolds developed the concept of the phytoplankton year for lake communities, separating succession from simple seasonality and calling the cyclical behaviour of environmental factors “periodicity” (Reynolds, 1980). Within the framework of neutral ecology (Hubbel, 2005) and lumpy coexistence theory (Scheffer and van Nes, 2006), numerical simulations have shown that phytoplankton community richness and succession are affected by the nature of resource fluctuations (gradual or sudden) (Roelke and Spatharis, 2015a, 2015b). Recently, Sakavara et al. (2018) also showed that assemblage-like structures occur numerically in a wide range of spectral modes of resource fluctuations.

The important role that coastal ecosystem characteristics play in the distribution of phytoplankton taxa has been highlighted for several coastal ecosystems (Harding, 1994; Brush et al., 2021). The cyclical behaviour of seasonal phytoplankton dynamics is considered one of the most obvious features of this influence (Mozetič et al., 1998; Cerino et al., 2019; Salgado-Hernanz et al., 2019). In particular, in the near-shore environment, the usual pattern of environmental factors is a short period of time with fluctuations on the order of 2 to 4 months (Winder and Cloern, 2010). This rate of fluctuation has been recently described as characteristic as well for the phytoplankton community in the northern Adriatic in agreement with the expected fluctuation rate of environmental parameters (Vascotto et al., 2021). Cyclic patterns for phytoplankton communities have been recognized for this area of the Mediterranean (Bernardi Aubry et al., 2012), but these communities have also been described as sensitive to erratic behaviour of environmental forces (Malej et al., 1997). Partial phase synchronization together with chaotic dynamics is a feature of biological populations in extensive ecological systems where diffusive migration is possible (Blasius et al., 1999). The northern Adriatic can be considered such an ecological system, as it is located in the meteorological mesoscale region (Orlanski, 1975) and its waters are connected by the main cyclonic circulation of the Northern Adriatic (Poulain et al., 2001; Petelin et al., 2013). On the other hand, recent studies of marine ecosystems suggest that phytoplankton diversity varies strongly within meso- and sub-mesoscale distances (10–100 km) and that large-scale environmental conditions have a relevant influence on assemblage formation (Levy

et al., 2015; Levy et al., 2018; Francé et al., 2021).

As we have seen so far, there is a gap between the theoretical models for the role of the cyclicity of environmental conditions in shaping succession (Reynolds, 2006) and formation (Sakavara et al., 2018) of phytoplankton assemblages with examples from the field (Vascotto et al., 2021). Furthermore, the complexity of patterns in phytoplankton phenology (Cloern and Jassby, 2010) does not allow for simple conclusions about the behaviour of multivariable objects such as phytoplankton assemblages. Nevertheless, it is crucial for the modelling of phytoplankton patterns to investigate in more detail the relationships between phytoplankton assemblages and environmental factors, their explanatory power and their harmonic properties. Our working hypothesis is that a model based on the regularity of mesoscale environmental factors can predict the structure and temporal distribution of the phytoplankton community when assemblages are used as the level of community organisation/composition in the analyses.

At two sampling stations of the northern Adriatic LTER (Long-Term Ecological Research) sites in the Slovenian part of the Gulf of Trieste (GoT) and the Italian Gulf of Venice (GoV) (Fig. 1), the phytoplankton community has been actively sampled for decades. The sites are located 100 km apart, thus ideal to study the synchronization between the phytoplankton community and environmental factors, and the extent of these relationships at the mesoscale. Since cyclic, seasonal, and periodic patterns all belong to the family of autocorrelation patterns, Tobler's first law applies: “*Everything is related to everything else, but near things are more related than distant things*” (Tobler, 1970). The analysis of autocorrelation patterns has emerged as a spatial technique in geographic studies, but from the analytical point of view, the use of time instead of space as a dimension of interest is equivalent (Legendre and Legendre, 2012).

In this work, we have studied the importance of autocorrelative processes in the northern Adriatic from the point of view of environmental forces in the time domain. We used the periodic and non-periodic components of these forces to model the time series of the phytoplankton community in the GoT on the eastern side of the northern Adriatic. We then attempted to extend the predictive capacity of our model to the western side of the northern Adriatic (GoV) at the boundary of the mesoscale domain.

2. Material and methods

2.1. Study area

The northern Adriatic basin is defined as the area north of the 100-m isobath of the Adriatic Sea and represents the largest shelf area in the Mediterranean Sea (Gačić et al., 2001). This basin is under the influence of intense lateral (river discharge and southward transport) and surface (wind and air temperature) stresses (Poulain et al., 2001). The water column of the northern Adriatic is seasonally mixed and stratified (Poulain et al., 2001), and in many areas the euphotic zone exceeds the depth of the upper mixed layer for most of the year (Talaber et al., 2014). The northern Adriatic is under the influence of two main winds, the “Bora” and the “Jugo” (Scirocco), the first blowing from the northeast and the second from the southeast. Bora is a strong katabatic wind that affects the water column in two ways: mixing and cooling, while Jugo is a constant wind with maximum speed in the eastern part of the basin and has a chaotic effect on the current circulation in the GoT (Malačić and Petelin, 2001).

The Slovenian LTER station (Fig. 1: 000F; 45.54 N, 13.55 E; 22 m depth) is located at the southern entrance of the Gulf of Trieste (GoT), which is a shallow basin with an average depth of 21 m (Malačić et al., 2006). The Italian LTER station (Fig. 1: AAOT, 45.32 N, 12.50 E, 16 m depth) is located offshore of the Venice Lagoon in the Gulf of Venice (GoV). Both gulfs are under the influence of freshwater (Zhang et al., 2020): GoT is influenced by the Soča River (Malačić and Petelin, 2001) and occasionally by the Po River plume (Vilicic et al., 2013), while GoV

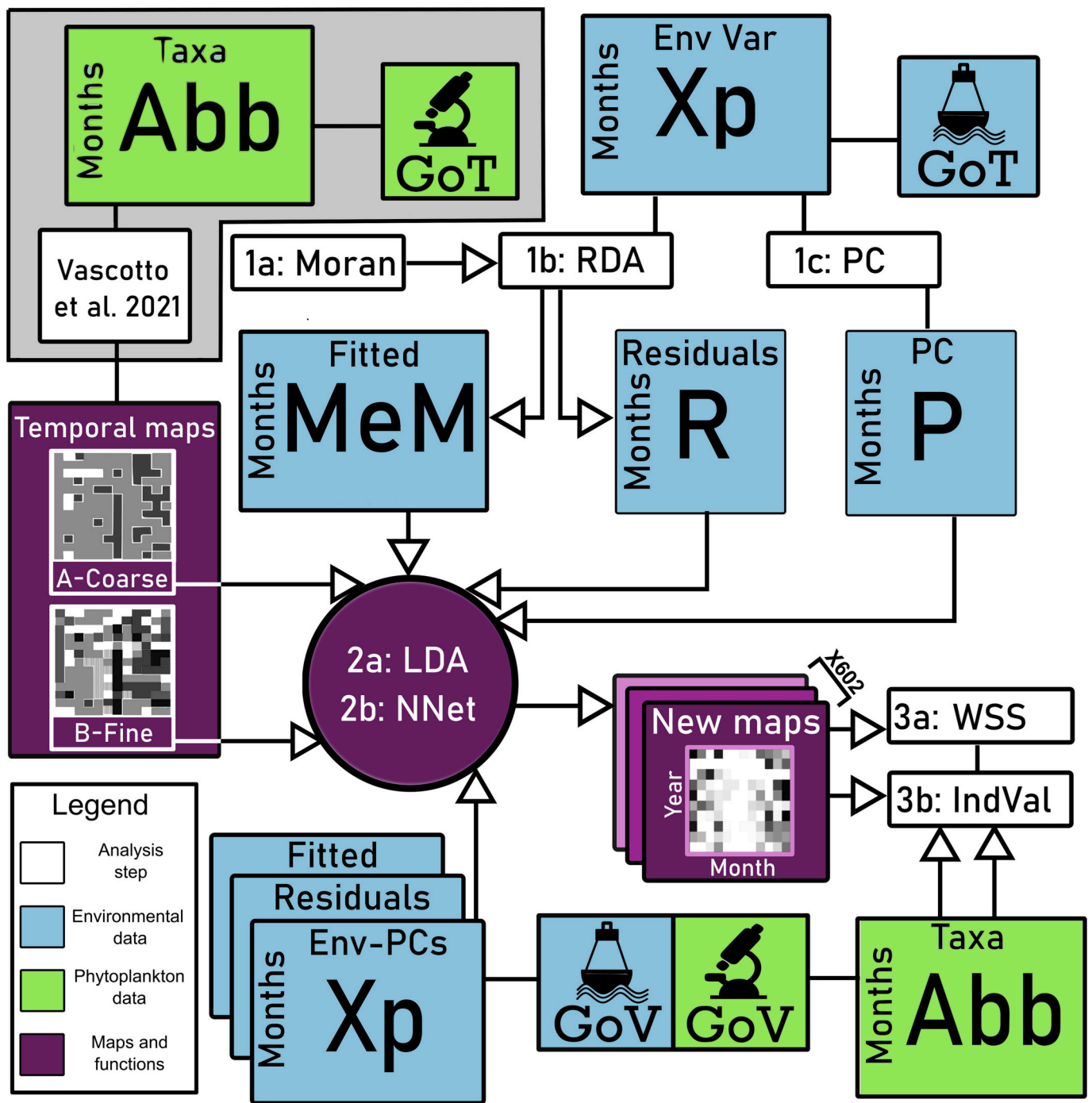


Fig. 2. Flowchart of the analysis. Each box represents either a data matrix, an analysis step, or the classification functions and temporal maps. In the boxes representing data matrices, the names of the variables and the names of the objects are given at the top and left of each box. In the boxes representing the analysis steps, the name of the analysis and the code used in the text are given to refer to it. In the upper left part of the diagram, the grey area contains all data and analyses already included in Vascotto et al., 2021. The temporal maps below the grey area represent the results of that analysis as well as the starting point for the present analysis. The circle represents both the linear discriminant analysis and the neural networks. Note that several arrows point to this circle area, but for each iteration of the analysis, the algorithm presented here uses only one of the two original maps (coarse or fine), only one of the three GoT environment matrices for training (MeM, R, or P), and only one of the three GoV environment matrices for prediction. Each of the 602 predicted temporal maps is then tested separately with GoV phytoplankton data (Abb).

is influenced by Po River plume (Poulain et al., 2001). Rivers like Tagliamento, Livenza, Piave, Brenta and Adige contribute to river discharge in northern Adriatic but, all together, they sum to only a minor fraction of the Po runoff (Cozzi and Gianì, 2011).

2.2. Data

A 12-year time series from 2005 to 2017 and comprising 130 taxa from station 000F (Fig. 1) was collected and stored as part of routine sampling in the Slovenian national monitoring programme. The data is produced on a monthly basis. Phytoplankton structure and abundance

Table 1

Environmental data used in the analysis: raw data, the operation applied to the raw data and the parameter obtained.

Original data	Operation	Parameter	Name
Rain (mm)	Cumulative sum	Rain	Rain
	Coefficient of variance	Rain variance	Rain_var
Temperature air (C)	Mean	Temperature	T_air
Temperature surface (C)	Mean(Surface-Bottom)/Depth	Thermocline strength	T_grad
Temperature bottom (C)			
River outflow (m ³ /s)	Mean	River	River
	Coefficient of variance	River variance	River_var
Salinity surface	Mean	Salinity	Sal
Wind speed (m/s)	Mean	Wind	Wind
Wind speed and direction (m/s, Θ)	Mean(speed*cos(Θ))	N.S. component	N.S.
Wind speed and direction (m/s, Θ)	Mean(speed*sin(Θ))	E.W. component	E.W.

data of station 000F were analysed in a previous study Vascotto et al. (2021) where a temporal maps of assemblages and their indicative taxa were obtained (Fig. 2: Temporal maps A and B, more information present in Supplementary material S16). From Vascotto et al. (2021) we had two possible partition systems available, a coarse phytoplankton assemblage partition (Fig. 2: Temporal map A) from which two main assemblages were used and a fine phytoplankton assemblage partition (Fig. 2: Temporal map B) from which six main assemblages were used. We reduced the number of assemblages from Vascotto et al. (2021) because only assemblages that covered at least six samplings/months were used. These phytoplankton assemblages were the starting point for the present analysis.

For the GoT, we also collected data on rain, wind direction and strength, salinity, air temperature, Soča river flow, sea surface and bottom temperature and stored them in an environmental table (Fig. 2: Xp). The data covered the same time period (2005–2017), more details are given in the Supplementary material S1. These data come from the oceanographic buoy Vida, located at a distance of 1.16 km from station 000F (wind, air temperature, water temperature and salinity; <https://www.nib.si/mbp/en/oceanographic-data-and-measurements/buoy-2>) and from the database of Slovenian Environment Agency (rain, river discharge; <https://www.arso.gov.si/en/>).

For the GoV, we also collected data on precipitation rain, wind direction and strength, salinity, air temperature, sea surface and bottom temperature form data collected onboard of Acqua Alta Oceanographic Tower (AAOT) by mean of WMO certified meteo station and Seabird SBE 19 CTD casts (Fig. 2: Xp). The environmental dataset covered the period between 2010 and 2019, more details are given in the Supplementary material S11. Phytoplankton structure and abundance data from the station AAOT covered the years from 2010 to 2018 and comprised >300 taxa (Fig. 2: Abb). The data was produced on a monthly basis.

The temporal density of the environmental data was on the order of hours, so we merged the data from the 30 days prior to each phytoplankton sampling to calculate the new variables as summarised in Table 1. The transformed data accounted for environmental conditions between phytoplankton sampling events.

The differences between the averages of the environmental parameters in the two sites were tested using a t.test, while the presence of linear trends was tested using the F-statistic of the Pearson R squared value (Legendre and Legendre, 2012).

2.3. Analysis

2.3.1. Decomposition of environmental data

Autocorrelation of environmental parameters was investigated using distance-based Moran eigenvector maps (Legendre and Legendre, 2012). We used the eigenvectors maps (Fig. 2: 1a Moran) to remove

significant autocorrelation components from the detrended GoT environmental data by performing a redundancy analysis (Fig. 2: 1b RDA) between relevant eigenvectors and environmental data (Legendre and Legendre, 2012). In this way, we generated two datasets: one with the fitted values containing the periodic component (Fig. 2: MeM) and the other with residuals containing the non-periodic part (Fig. 2: R). Moreover, we calculated the global Moran's I to estimate the autocorrelation for each environmental variable (Legendre and Legendre, 2012). Finally we used the variation partitioning approach (Legendre and Legendre, 2012) to assess the power of GoT environmental components in explaining the variance of the GoV environmental data, that have been decomposed in periodic and non-periodic components prior the variation partitioning analysis. We used the R package "adespatial" (Dray et al., 2016) to compute the eigenvectors maps and the Moran's I of each environmental parameter. We used the R package "vegan" (Oksanen et al., 2013) to apportioning the variation among GoT and GoV components and to produce the resulting Venn diagrams.

Apart from periodic and non periodic components of the environmental data, also the complete environmental dataset was used after the decomposition with principal component analysis (Fig. 2: 1c PCA). From the three environmental datasets, the first three principal components were retained (Fig. 2: MeM, R, P). The use of the three first axes was dictated by the small number of objects to model in certain assemblages.

Modelling the relationship between environment and phytoplankton assemblages.

To examine linear relationships between the phytoplankton assemblage partitions (coarse and fine) obtained from Vascotto et al. (2021) in form of an occurrence vector and all three environmental datasets (MeM, R, P), we used linear discriminant analysis (Fig. 2: 2a LDA). The significance of these relationships was evaluated using Wilks Λ (Legendre and Legendre, 2012). The discriminant functions obtained from the LDA of both partitions were then used to reclassify the objects of each assemblage and evaluate the success rate of these functions.

The environmental parameters from GoV were analysed following the same procedure (Fig. 2: Xp) to obtain the complete, periodic and non periodic environmental datasets. The statistically significant LDA discriminant functions obtained in GoT (Wilks Λ with $p < 0.05$) were then applied to forecast the presence of phytoplankton assemblages in GoV using the corresponding environmental dataset from GoV.

To overcome the linearity constraints of LDA analysis, we used Neural networks (Fig. 2: 2b NNet) modelling approach. Also here, the NNets were trained on complete, periodic and non periodic environmental datasets with coarse and fine phytoplankton assemblage partitions from GoT. The resulting six classification functions were used to forecast phytoplankton assemblages in GoV using the corresponding environmental datasets (Fig. 2: Xp). The six parallel tests were each repeated 100 times. The training-to-test ratio was 80–20 %. The NNets were built using the TensorFlow package (Abadi et al., 2015) in Python 3.8. The architecture of the NNets consisted of three layers enabled by linear rectifiers (ReLU) and softmax function. The search optimization algorithm (Adam) attempted to minimise cross entropy by using L1 and L2 regularizations to avoid overfitting.

To characterize each assemblage in terms of environmental conditions for both GoT and GoV, we calculated the average value of environmental parameters and their variances in the samples/months representing a certain assemblage. The environmental parameters were represented as standardized values in bar plots.

2.3.2. Evaluation of phytoplankton assemblages

To evaluate the forecasted assemblages in GoV, we calculated the IndVal index with the corresponding p -value (Fig. 2: 3b IndVal) on the GoV phytoplankton community data (Fig. 2: Abb). The IndVal is an index that takes into account the fidelity and the specificity of a certain taxon in a cluster of samples (Dufrene and Legendre, 1997). In our case it was calculated for taxa in the forecasted phytoplankton assemblages resulting from the statistically significant LDA classification functions

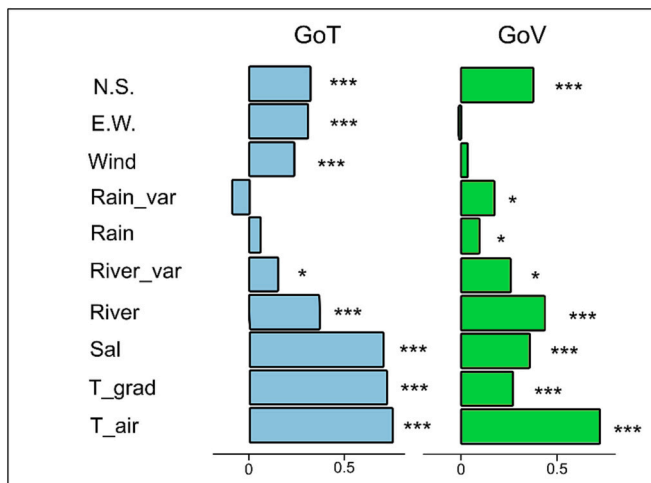


Fig. 3. Global Moran's I for the environmental data in GoT and in GoV. The significance of each value is encoded with stars: * correspond to significant Moran's I (p-value <0.05), *** correspond to highly significant results (p-value <0.01).

(2) and all NNet classification functions (600) (Fig. 2: New Maps). The average p-value of IndVal was used to score each forecasted phytoplankton assemblages. In parallel, we also calculated the within-group sum of squares (WSS) over the chi-square transformed matrix of abundances (Legendre and Legendre, 2012). The chi-square values represent the deviations of a certain taxon in a sample from its expected abundance while the WSS represents the homogeneity of such values inside the clusters of samples. Values close to one indicate a poor classification of the samples variance, in this case taxa deviations, while values close to zero would indicate a perfect classification of the variance. IndVal p-values and WSS values for the six parallel outcome groups (coarse and fine phytoplankton assemblage partitions per complete, periodic and non periodic components of environmental datasets) were represented with box-plots and differences tested with the Kruskal-Wallis test. Pairwise differences were tested for significance using the Tukey-Kramer test for independent samples. The forecasted assemblages obtained using the complete environmental dataset were chosen to be explored further in the discussion since they represented the best possible predictions.

3. Results

3.1. Environmental conditions

The environment in the two neighbouring areas in the northern Adriatic was relatively stable during the study period. Of the 10 variables considered in GoT and in GoV, none showed a positive or negative long-term trend, with the exception of the mean discharge of the Soča River in GoT which showed a slightly positive trend (Supplementary material S 5). With respect to the average values, some environmental parameters were significantly different at the two sites. The thermocline appeared to be stronger in GoV (0.193 °C/m on average) than in GoT (0.130 °C/m) (p-value <0.01), and the water in GoV was less salty (34.1 vs 36.6, p-value <0.01). In addition, the Po River discharge and its coefficient of variance were higher than the Soča river discharge. On the contrary, air temperature, wind speed, rain and its coefficient of variance were similar in the two sites (p-value >0.05). The wind roses of wind speed and direction (Supplementary materialS6) indicate that the main winds in the GoT had a strong NEE contribution and a secondary component from the south (S and SSE). Winds in the GoV also had a large contribution from the northeast quadrant (NNE and NE) and secondary components from the southern quadrants.

Most environmental variables exhibited some degree of periodicity

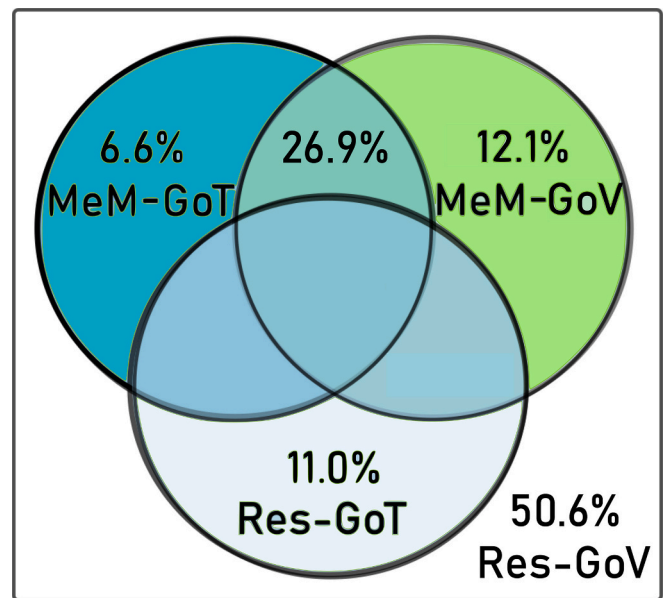


Fig. 4. Venn diagram of the variance partition of the environmental dataset from GoV. Variance is partitioned between the two periodic components of the two environments (MeM-Got and MeM-GoV) and the residuals of the environmental variables from GoT (Res-GoT). The intersections with no value represent zero or negative values which together with the remaining values sum up to 100 %.

in both study areas (Fig. 3). Overall, periodicity explained a relevant proportion of the variance in environmental data (46 % in GoT and 39 % in GoV- More details are given in the Supplementary material). Periodicity in environmental parameters was less pronounced in GoV compared to GoT, as indicated by generally lower Moran's I in Fig. 3. In GoT, three parameters, i.e. salinity, air temperature, and thermocline strength, showed the most pronounced cyclic behaviour, while rain and rain variability seem to show mainly erratic behaviour. On the contrary, the rain pattern was somewhat more regular in GoV. In addition, in GoV the average wind speed and the strength of the east-west components showed a more pronounced erratic behaviour. The same was true for the thermocline and salinity.

The combination of the periodic components from GoV (Fig. 4: MeM-GoV) and from GoT (Fig. 4: MeM-GoT) explained 45.6 % of the variance in the GoV environmental data. The periodic components of GoV and GoT shared ~26.9 % of the explained variance. The remaining variance was partially explained (11.0 %) by the non-periodic components of the environmental data from GoT (Fig. 4: Res-GoT). The residual variance (Res-GoV 50.6 % in Fig. 4) corresponds to the variance of local non-periodic events.

Table 2

Results of LDA on the two phytoplankton assemblage partitions from Vascotto et al. (2021) with three different environmental datasets from GoT. The bold values correspond to LDA configuration that resulted significant (p-value < 0.05).

Phytoplankton assemblage partition from Vascotto et al. (2021)	Environmental dataset	Wilks Λ	p-value
Coarse (2 assemblages)	Complete (principal components)	0.98	0.69
	Periodic component	0.96	0.33
	Non-periodic component	0.97	0.51
Fine (6 assemblages)	Complete (principal components)	0.73	0.0037
	Periodic component	0.67	0.001
	Non-periodic component	0.87	0.25

Table 3

The efficiency of the LDA and NNets in reclassification in % of correctly classified GoT objects. In the second column the original encoding from Vascotto et al., 2021 are reported in order to facilitate the comparison. The results refer to the reclassification obtained using the complete environmental dataset.

Assemblage	Original encoding	LDA	NNets
A	Group IX	4 %	40 %
B	Group IV	70 %	92 %
C	Group XI	13 %	66 %
D	Group XII	0 %	70 %
E	Group III	75 %	100 %
F	Group VII	67 %	78 %
Weighted mean		21 %	60 %

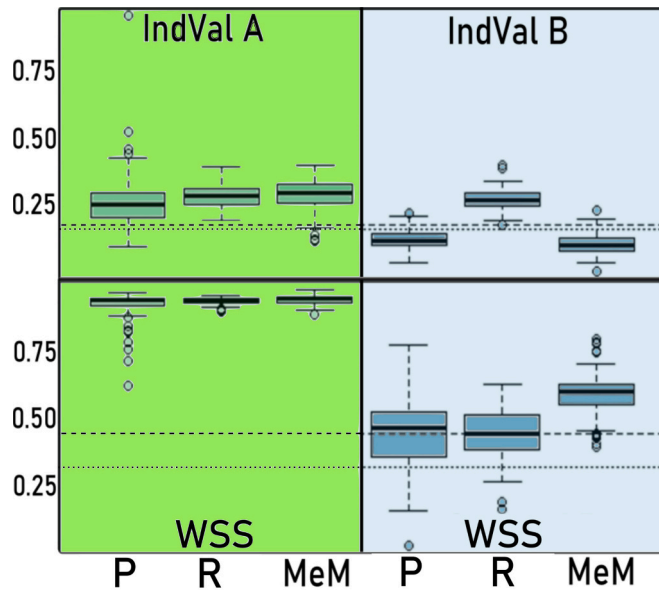


Fig. 5. Boxplots of average IndVal p -values (upper panel) and WSS values (lower panel) for the Neural network predicted phytoplankton assemblages in GoV. The green left panel represents the results obtained from the coarse phytoplankton assemblage partition from Vascotto et al. (2021), blue right panel refers to results obtained from fine phytoplankton assemblage partition from Vascotto et al. (2021). Each panel includes from left to right the results got using complete environmental dataset (P), its non periodic (R) and periodic component (MeM). Horizontal lines in the right panel represent the average IndVal p -value and WSS for the assemblages predicted with two statistically significant discriminant functions of the LDA: Dotted lines represent the predicted assemblages with complete environmental dataset, dashed lines represent the predicted assemblages with periodic component.

3.2. Efficiency of linear and non-linear classification functions for predicting phytoplankton assemblages

From the results of Vascotto et al. (2021) only assemblages present at least in six months were retained from further analysis. This corresponded to two assemblages from the coarse partition and six from the fine one. The six assemblages covered 128 months of the total 152 we had at our disposal. No significant linear relationship with environmental variables in GoT was found when performing linear discriminant analysis (LDA) with two assemblages from the coarse phytoplankton assemblage partition, neither with complete environmental dataset nor with data decomposed in periodic and non-periodic components (Table 2). On the contrary, when using the fine phytoplankton assemblage partition from Vascotto et al. (2021), the six assemblages discriminated a relevant part of the variance of the principal components of the complete environmental dataset and of its periodic part while there was no relationship with the non-periodic component of the

environmental dataset (Table 2).

However, the classification functions obtained from the LDA with two statistically significant settings (for complete environmental dataset and periodic component) were only able to correctly reclassify on average 21 % of the objects in the associated assemblages. But, when looking at the reclassification results at the level of single assemblage, the success of correct classification was quite high for 3 assemblages and very low for the remaining 3 (Table 3). The Neural Networks (NNets) were able to correctly reclassify on average 60 % of the objects using its non-linear classification functions (Table 3). For the three assemblages for which LDA performed poorly (A, C, D) the reclassification of the NNets is greatly improved.

3.3. Evaluation and composition of predicted phytoplankton assemblages in Gulf of Venice

Both classification functions resulted from LDA (only from the two statistically significant settings; see Table 2) and from Neural networks (from all six settings) on GoT data were used to forecast the assemblages in GoV. We first present the evaluation of the predicted phytoplankton assemblages within the coarse and the fine phytoplankton assemblage partition by neural networks, using the mean IndVal p -values and WSS values obtained with the complete environmental dataset (Fig. 5, P) and with its periodic (Fig. 5, MeM) and non-periodic components (Fig. 5, R). For both IndVal p -values and WSS, the differences between the six groups were significant (Kruskal-Wallis test; p -value <0.001). The IndVal p -values and the WSS values we obtained from the coarse phytoplankton assemblage partition (Fig. 5, left) were generally higher than those obtained from the fine phytoplankton assemblage partition (Fig. 5, right). While there were no substantial differences between the three cases (P, R and MeM) within the coarse phytoplankton assemblage partition (Fig. 5, left), a different pattern emerged within the group of fine phytoplankton assemblage partition (Fig. 5, right). The IndVal p -values obtained using complete environmental dataset (Fig. 5: IndVal B, P) and its periodic components (Fig. 5: IndVal B, MeM) were significantly lower than those obtained using the non-periodic component (Fig. 5: IndVal B, R) (Tukey-Kramer test; p -value <0.001). In the case of evaluation with the WSS values, they were significantly higher for the assemblages obtained with periodic component of environmental data (Tukey-Kramer test; p -value <0.001).

In comparison, the mean IndVal p -values of assemblages predicted by LDA discriminant functions (Fig. 5; horizontal lines in right upper panel) were lower than those obtained by neural network either for the coarse phytoplankton assemblages or for the fine phytoplankton assemblages using the non periodic component. The mean WSS values (Fig. 5; horizontal lines in right lower panel) indicate that the results for the assemblages predicted by LDA using the complete environmental dataset are better than those using its periodic part, mirroring the results from neural networks.

The best results in terms of average p values were obtained for the assemblages predicted by neural networks using the periodic components, although no significant difference was found in comparison to the results from the complete environmental dataset (Fig. 5; IndVal B, P and MeM). On the contrary, from the point of view of WSS the assemblages predicted by neural network using the complete dataset performed better than those using the periodic components (Tukey-Kramer test; p -value <0.001). Therefore, as the best synthesis the assemblages predicted for GoV by neural network with the use of the complete environmental dataset is further analysed in the following.

In Fig. 6, the similarities, and differences between the “original” phytoplankton assemblages (GoT) and those predicted for GoV are presented together with the environmental conditions. Assemblages are presented as clusters of sampling dates characterised by certain phytoplankton taxa (Fig. 6, temporal maps). Environmental conditions associated to these assemblages are presented as standardized average values of environmental parameters and their variances in the samples/

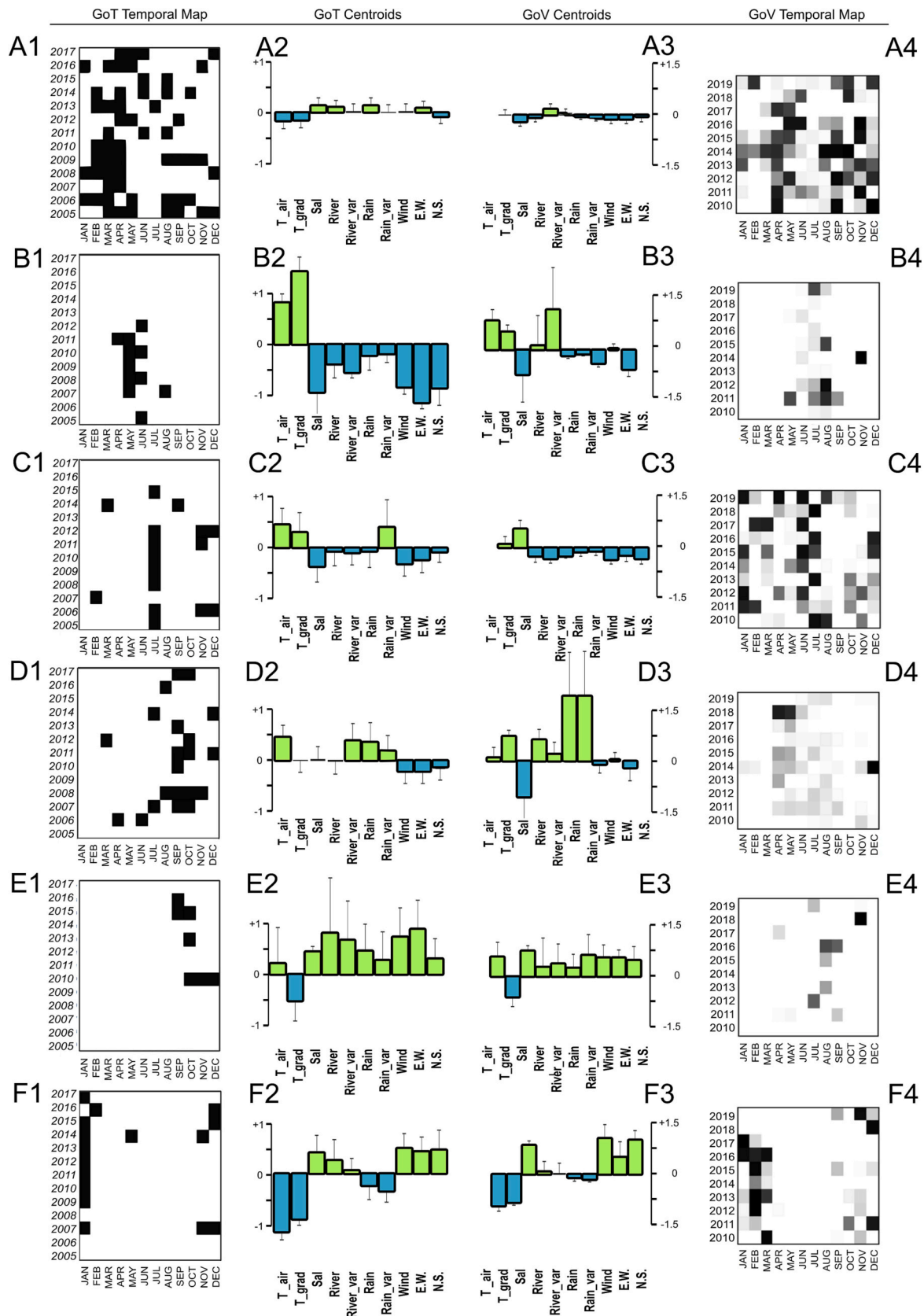


Fig. 6. Phenology of the six phytoplankton assemblages and the corresponding environmental conditions. A1-F1: temporal distribution of phytoplankton assemblages in GoT (from Vascotto et al., 2021); A2-F2: environmental characteristic in GoT; A3-F3: environmental characteristic in GoV; A4-F4: temporal distribution of predicted phytoplankton assemblages in GoV. The bar charts represent environmental variables in standardized values (mean + sd). Note the different scales on y axes. The temporal maps for GoV and GoT are expressed in probability (darker the colour, the higher the probability that a certain month belongs to an assemblage). The temporal map of GoT had probability either 0 or 1 having been already defined at the beginning of the study.

Table 4

The indicative taxa of phytoplankton assemblages. For GoT the indicative taxa are represented by the IndVal (from Vascotto et al., 2021). An IndVal value >0.2 is a sign of indicativity for a certain assemblage. Taxa are ordered in decreasing order of IndVal. For GoV, only taxa with the highest IndVal values are shown.

GoT		GoV	
Taxa	IndVal	Taxa	IndVal
A			
Cryptophyceae	0.08	Coccolithophyceae	0.34
Phytoflagellates	0.06	<i>Lessardia elongata</i>	0.29
Prasinophyceae	0.06	<i>Diplopsalis</i> group	0.28
<i>Meringosphaera mediterranea</i>	0.05	<i>Chaetoceros diversus</i>	0.23
<i>Prorocentrum cordatum</i>	0.05	<i>Leptocylindrus danicus</i>	0.23
<i>Gymnodinium</i> spp.	0.05	<i>Protopteridinium steinii</i>	0.23
Chlorophyceae	0.04	Dinophyceae	0.22
<i>Gyrodinium</i> spp.	0.03	<i>Amphora</i> spp.	0.20
<i>Ophiaster hydroideus</i>	0.03	<i>Paulinella ovalis</i>	0.20
B			
<i>Cyclotella</i> spp.	0.44	<i>Cyclotella</i> spp.	0.42
<i>Prorocentrum gracile</i>	0.20	<i>Cyclotella caspia</i>	0.38
<i>Prorocentrum cordatum</i>	0.13	<i>Eutreptia lanowii</i>	0.37
<i>Chaetoceros simplex</i>	0.13	<i>Calciosolenia brasiliensis</i>	0.28
Prasinophyceae	0.12	<i>Dactyliosolen fragilissimus</i>	0.24
<i>Heterocapsa</i> group	0.11	<i>Tripos fusus</i>	0.23
C			
<i>Proboscia alata</i>	0.45	<i>Thalassionema nitzschioides</i>	0.56
<i>Chaetoceros</i> spp.	0.38	<i>Chaetoceros</i> spp.	0.31
<i>Rhizosolenia</i> spp.	0.19	<i>Emiliania huxleyi</i>	0.28
<i>Hemiaulus hauckii</i>	0.13	<i>Cerataulina pelagica</i>	0.26
<i>Thalassionema nitzschioides</i>	0.11	<i>Thalassiosira</i> spp.	0.26
Euglenophyceae	0.11	<i>Leptocylindrus minimus</i>	0.22
<i>Nitzschia</i> spp.	0.10	<i>Nitzschia longissima</i>	0.22
<i>Guinardia striata</i>	0.09	<i>Pseudo-nitzschia delicatissima</i> group	0.22
Phytoflagellates	0.07	<i>Chaetoceros affinis</i>	0.21
<i>Gymnodinium</i> spp.	0.07	<i>Bacteriastrium</i> spp.	0.20
D			
<i>Nitzschia</i> spp.	0.14	<i>Pyramimonas</i> spp.	0.33
<i>Guinardia striata</i>	0.12	<i>Ebria tripartita</i>	0.28
<i>Dactyliosolen fragilissimus</i>	0.10	<i>Calcidiscus leptoporus</i>	0.27
<i>Syracosphaera pulchra</i>	0.09	<i>Leucocryptos marina</i>	0.25
<i>Hemiaulus hauckii</i>	0.09	<i>Prorocentrum gracile</i>	0.25
Coccolithophyceae	0.09	<i>Prorocentrum cordatum</i>	0.24
<i>Proboscia alata</i>	0.07	<i>Cocconeis scutellum</i>	0.23
<i>Rhabdosphaera stylifera</i>	0.06	Cryptophyceae	0.23
Phytoflagellates	0.06	<i>Chaetoceros simplex</i>	0.21
<i>Pseudo-nitzschia delicatissima</i> group	0.06	<i>Protopteridinium</i> spp.	0.21
E			
<i>Pseudo-nitzschia delicatissima</i> group	0.65	<i>Gyrodinium spirale</i>	0.77
<i>Nitzschia</i> spp.	0.28	<i>Gyrodinium</i> spp.	0.51
<i>Syracosphaera pulchra</i>	0.28	<i>Cochlodinium</i> sp.	0.47
<i>Calciosolenia murrayi</i>	0.24	<i>Guinardia striata</i>	0.45
<i>Dactyliosolen fragilissimus</i>	0.20	<i>Torodinium robustum</i>	0.42
<i>Gyrodinium</i> spp.	0.18	<i>Nitzschia sigma</i>	0.35
<i>Tripos fusus</i>	0.18	<i>Oxytoxum</i> spp.	0.31
<i>Calciosolenia brasiliensis</i>	0.17	<i>Pleurosigma</i> spp.	0.31
<i>Ophiaster hydroideus</i>	0.16	<i>Psammodictyon panduriforme</i>	0.31
<i>Rhizosolenia</i> spp.	0.13	<i>Pseudo-nitzschia seriata</i> group	0.31
<i>Tripos furca</i>	0.13	Bacillariophyceae	0.30
<i>Pseudo-nitzschia seriata</i> group	0.11	<i>Chaetoceros curvisetus</i>	0.29
Euglenophyceae	0.10	<i>Gymnodinium</i> spp.	0.29
<i>Prorocentrum triestinum</i>	0.10	<i>Chaetoceros danicus</i>	0.28
<i>Guinardia striata</i>	0.08	<i>Dactyliosolen blavyanus</i>	0.28
<i>Rhabdosphaera stylifera</i>	0.08	<i>Hemiaulus hauckii</i>	0.28
<i>Gymnodinium</i> spp.	0.08	<i>Hermesinium adriaticum</i>	0.28
<i>Gonyaulax</i> spp.	0.08	<i>Katodinium glaucum</i>	0.28
<i>Leptocylindrus mediterraneus</i>	0.07	<i>Paralia sulcata</i>	0.28
<i>Cerataulina pelagica</i>	0.07	<i>Proboscia alata</i>	0.26

Table 4 (continued)

GoT		GoV	
Taxa	IndVal	Taxa	IndVal
<i>Proboscia alata</i>	0.07	<i>Heterocapsa</i> group	0.25
<i>Heterocapsa</i> group	0.07	<i>Nitzschia</i> spp.	0.23
<i>Emiliania huxleyi</i>	0.07	<i>Chaetoceros decipiens</i>	0.22
<i>Pleurosigma normanii</i>	0.06	Phytoflagellates	0.22
<i>Diploneis crabro</i>	0.06	<i>Guinardia flaccida</i>	0.21
Cryptophyceae	0.06	<i>Rhizosolenia imbricata</i>	0.21
F			
<i>Emiliania huxleyi</i>	0.11	<i>Skeletonema costatum</i> s.l.	0.35
<i>Ophiaster hydroideus</i>	0.07	<i>Dictyocha fibula</i>	0.29
<i>Diploneis crabro</i>	0.07	<i>Asterionellopsis glacialis</i>	0.29
Prasinophyceae	0.06	<i>Diploneis crabro</i>	0.25
<i>Meringosphaera mediterranea</i>	0.06	<i>Dactyliosolen phuketensis</i>	0.21

months occupied by the assemblage (Fig. 6, env. centroids). For the predicted phytoplankton assemblages in GoV, the indicative taxa are presented with the appertaining IndVal index (Table 4). The indicative taxa of phytoplankton assemblages in GoT are presented by IndVal (Table 4, from Vascotto et al., 2021).

The first phytoplankton assemblage we describe (Fig. 6, A1) was originally defined as the base community in GoT (Vascotto et al., 2021). This and the remaining assemblages of GoT were defined on the basis of the community composition following the method described in Supplementary material in S 16. It is scattered during whole time-series but more concentrated in the first half of the year. The predicted phenology for this assemblage in GoV was similar to that in GoT in that it occurred throughout the year (Fig. 6, A4). Another similarity concerns the fact that in both GoT and GoV this assemblage had a mix of indicative taxa from different phytoplankton classes. While in GoT these were mostly belonging to the phytoflagellates, in GoV most indicative taxa were coccolithophores, diatoms and dinoflagellates (Table 4, A). In both areas, the environmental conditions for this assemblage were characterised by parameters fluctuating around the overall mean, but with standardized values not exceeding ± 0.20 .

In GoT, the spring phytoplankton assemblage (Fig. 6, B1) was mainly characterised by the presence of diatom *Cyclotella* spp. and small dinoflagellates of the genera *Prorocentrum* and *Heterocapsa* (Table 4, B). This assemblage was present in stratified waters (T_grad standardized average at 1.24 from the overall mean) with low surface salinity (standardized average at -0.75), relatively high air temperature (standardized average at 0.71) and weak winds. Using the classification functions obtained by neural networks, the presence of this assemblage in GoV was predicted mainly for late spring-late summer period. Environmental conditions for this predicted assemblage were partly similar to those in GoT, with stratified (T_grad standardized average at 0.55) and warm (T_air standardized average at 0.90) waters, but with an important contribution of river discharge variability (River_var standardized average at 1.23). Also in the predicted assemblage, the most indicative taxa belonged to the genus *Cyclotella* (Table 4, B).

The third phytoplankton assemblage in GoT (Fig. 6, C1) represents a predominantly diatom assemblage (Table 4) with most occurrences in July but also in other seasons. The predicted phenology of this assemblage in GoV also indicates a scattered distribution throughout the year although the highest probability of occurrence was in summer months (Fig. 6, C4). Also here, the assemblage was dominated by the presence of diatoms (Table 4, C). Environmental conditions in both areas (Fig. 6, C2 and C3) were similar to those during the previous assemblage (B2) but with less pronounced values of parameters' standardized averages. In addition, there was also an important contribution of rain variability in GoT (standardized average at 0.35); while river discharge variability was not so important for this assemblage in GoV.

The fourth phytoplankton assemblage in GoT presented in Fig. 6 (D1) occurred primarily in the second half of the year, mainly in autumn and

was characterised by a mix of coccolithophores and large centric diatoms (Table 4, D). This assemblage could be easily associated with warmer periods under the influence of pulsating freshwater inputs due to rivers and rain (Fig. 6, D2). In GoV, the phenology of the predicted phytoplankton assemblage was different and characterised mainly by low probability of occurrence (Fig. 6, D4). The environmental conditions were mainly determined by exceptionally high values of rain (Rain standardized average at 1.99, Rain_var standardized average at 2.13, Fig. 6, D3). This assemblage differed from the original not only in its phenology but also in terms of indicative taxa, since here the contribution of phytoflagellates was substantial (Table 4, D).

The autumn in GoT was characterised also by another phytoplankton assemblage (Fig. 6, E1) which was defined by the presence of pennate diatoms, coccolithophores and thecate dinoflagellates (Table 4, E). This assemblage was only present from 2010 onwards and was delineated by well-mixed water column (T_grad standardized average at -0.45), with high river outflow (River standardized average at 0.72 and strong winds with E-W component (E-W standardized average at 0.78) (Fig. 6, E2). The occurrence of such assemblage in GoV was predicted for late summer-early autumn (Fig. 6, E4), with environmental conditions similar to that in GoT: mixed water column (T_grad standardized average at -0.63), relatively warm weather (T_air standardized average at 0.60) and high salinity (sal standardized average at 0.78) and strong winds (Fig. 6, E3). This predicted assemblage was associated with a long list of indicative taxa (Table 4, E) of predominantly naked forms of dinoflagellates and diatoms. Coccolithophores were not indicative for this assemblage in GoV.

Coccolithophores *Emiliania huxleyi* and *Ophiaster hydroideus* together with small diatoms dominated the winter assemblage in GoT (Table 4, F). This assemblage occurred primarily in December and January (Fig. 6, F1) and was associated with cold weather (T_air standardized average at -0.96) and mixed water column (T_grad standardized average at -0.86) most likely associated to strong winds (Wind standardized average at 0.43, E-W standardized average at 0.38, N-S standardized average at 0.40) (Fig. 6, F2). A very similar pattern of environmental conditions emerged for the predicted assemblage in GoV (Fig. 6, F3), which also shared a similar phenology (Fig. 6, F4). The associated taxa in GoV (Table 4, F) were dominated by the diatom *Skeletonema costatum* s.l. and lacked the presence of coccolithophores characteristic for GoT. A benthic diatom *Diploneis crabro* was indicative of the winter community in both areas.

4. Discussion

4.1. Considerations on data representativeness

In a highly variable environment such as the northern Adriatic, which is prone to rapidly changing small scale conditions (Jeffries and Lee, 2007), it is probable that at the scale of a hundred km (distance between the LTER stations) these conditions would be different. However, the two locations have been described in several regionalization studies belonging to the same recognizable space, which can be distinguished by its abiotic characteristics and associated biological assemblage (Ayata et al., 2018). To study the influence of environmental parameters and their variability on the phytoplankton community in the two study areas, it was crucial to take into consideration the representativeness of the environmental data. These were collected from the source closest to phytoplankton sampling stations: at the LTER station itself for some parameters and at the nearest meteorological station for others. The reason we chose to use environmental data from a single site closest to LTER was double. First, in this way we avoided the “fading” of localized extreme events as would come from averaging multiple sites over larger area. Second, data from more distant sites could have blurred environmental cycles by adding out-of-phase patterns. Because the goal of this study was to assess the importance of cyclic patterns of environmental parameters in shaping the phytoplankton community, we

preferred the risk of underestimating the strength of these patterns to the opposite. Moreover, in this way, local extreme events and their influence on the model could also be taken into consideration.

Another consideration goes to the choice of environmental parameters, since the data we have used for the present analysis (some physical, meteorological and hydrological data) do not represent the totality of factors that influence the phytoplankton community in the northern Adriatic, e.g. physical, chemical and biological factors (Brush et al., 2021; Neri et al., 2022). The choice of parameters in this study was guided by the sufficient temporal frequency of data acquisition. At both LTER stations, the chemical parameters (i.e. nutrient concentrations) are sampled along with phytoplankton on a monthly basis, which poses two problems. First, the data represent the chemical status at the current time, and second, they are strongly influenced by randomness and measurement errors because of their small number. Since the rate of change of environmental parameters is higher than the rate of fluctuations in phytoplankton community (Hutchinson, 1941), using parameters from the day of sampling cannot provide a reliable picture of past conditions that determined a particular community. On the other hand, hydrological and meteorological data have the advantage of being recorded very frequently allowing to summarise the data over longer period (for example one month). In addition, most of the chosen data are indirect indicators of other relevant parameters, such as water column stability (T, salinity) and nutrient enrichment (river discharge and rain).

4.2. Patterns of mesoscale connectivity

Half of phytoplankton assemblages in GoT have been quite well characterised by linear relationships with the environmental parameters. Neural network improved the proportion of correct reclassifications in all six phytoplankton assemblages in GoT, indicating the existence of non-linear elements in the relationships between environment and phytoplankton, as well. The fact that the neural network was able to predict assemblages in GoV with similar indicative taxa indicates that these methods can be successfully applied to predict phytoplankton community structure at the mesoscale.

For assemblages with linear relationships, it was possible to find matching assemblages in GoV accompanied with similar or very similar environmental conditions. These assemblages were characterised, at least to some degree, by the same or related species in both environments. The assemblage that was in both areas dominated by *Cyclotella* species was characterised by a warm period and stratified water column. However, in GoV this assemblage was not predicted for late spring as in GoT, but mainly for summer and late summer. This phenological difference highlights the link between indicative taxa and environmental conditions, since the two assemblages are out of phase in both areas, but form under similar environmental conditions. However, besides thermal stratification also Po River discharges played a significant role for the formation of this assemblage in GoV.

Very similar environmental conditions and slightly different timing were characteristic also for the assemblage E. While in GoV this community was still dominated by diatoms, and dinoflagellates were characteristic for both areas, coccolithophores were exclusively typical for GoT. Such a rich and diverse community without a single dominant taxon is typical for the early autumn in the northern Adriatic (Bernardi Aubry et al., 2012; Marić et al., 2012; Cerino et al., 2019). One common element in both areas was the presence of species from the genus *Pseudo-nitzschia*, which are frequently mentioned as community-forming in the northern Adriatic (Marić et al., 2012; Godrić et al., 2013; Cerino et al., 2019). However, *Pseudo-nitzschia* species were also present in other assemblages, such as D in GoT and C in GoV, indicating the opportunistic nature of this genus (Bernardi Aubry et al., 2012). Within the present study *Pseudo-nitzschia* species were just assigned into two groups, i.e. the *P. seriata* and the *P. delicatissima* group, which could have contributed to uncertainties in defining indicative taxa and their niches (Turk Dermastia et al., 2020).

Differently from the described out-of-phase conditions for the “*Cyclotella*” and “*Pseudo-nitzschia*” assemblage, the late autumn-winter period in GoT and GoV was similar in terms of environmental conditions (cold period, mixed water column, strong winds) and temporally synchronized. Although the indicative taxa for this assemblage were mainly different for the two areas, most of them are considered as characteristic for the autumn-winter period in the northern Adriatic basin (Bernardi Aubry et al., 2012; Marić et al., 2012; Godrijan et al., 2013; Cerino et al., 2019). The common presence of the benthic diatom *Diploneis crabro* is in line with the phenology of the genus *Diploneis* described previously in the area (Cibic et al., 2012) and can be explained in light of the mixed condition present in winter. Also, *Skeletonema costatum* s.l. and *Asterionellopsis glacialis* were found to be typical for a few assemblages in GoT that were not included in the model, but occurred under the same environmental conditions as the winter cluster F1 (Vascotto et al., 2021). *S. costatum* s.l., which was the most indicative taxon for the winter in GoV, is considered to be responsible for the winter-early spring bloom across whole northern Adriatic (as *S. marinoi*), with increasing abundances towards its western part (Marić Pfannkuchen et al., 2018). However, the abundance of *S. costatum* s.l. decreased markedly in the GoT from 2013 onwards (Cerino et al., 2019; Vascotto et al., 2021). As concerns the coccolithophore *Emiliania huxleyi*, the main winter indicative species in GoT (Cabrini et al., 2012; Cerino et al., 2019; Vascotto et al., 2021), there was a recent decrease of its abundances in southern parts of the basin (Totti et al., 2019). It appears that winter conditions constitute a spatially uniform habitat at the mesoscale of the northern Adriatic and set favouring conditions for some common indicative taxa.

Fairly well temporally defined assemblage of relatively large, mostly colonial diatoms in the GoT formed also during summer (mainly in July) although with some appearance in winter and autumn too, but its appertaining environmental characteristics were not as good defined by linear discriminants as with previously discussed assemblages. Here, neural network significantly improved the predicting capacity and modelled a similar diatom dominated assemblage in GoV. Differences in phenology of this assemblage in the two areas can be justified by the underlying trophic differences. While in the GoV diatoms dominate the phytoplankton community most of the time (Bernardi Aubry et al., 2012) which was also predicted in our study, a recent July diatom peak has established in the GoT (Mozetić et al., 2012) and eastern part of the northern Adriatic (Marić et al., 2012), apparently governed by summer rain events. In GoT, a mixed community of nanoplanktonic phytoflagellates from different taxonomic groups predominantly dominates the phytoplankton community (Brush et al., 2021; Vascotto et al., 2021). The assemblage depicting this was the largest one considered in this study with indicative taxa from all groups. An assemblage with similar characteristics was predicted also for GoV, especially for spring and autumn, when also previous studies depicted a codominance among diatoms and other groups (Bernardi Aubry et al., 2012).

The last assemblage we discuss was found with a very different phenology and taxa composition in both areas. In GoT, this assemblage formed in conditions with relatively high rain and freshwater discharge pulses, which enriched the water column with nutrients and led to proliferation of large diatoms (Vascotto et al., 2021). On the contrary, a similar assemblage could not be predicted for GoV, where only three sampling dates were assigned with high probability to this group. These three sampling dates were characterised by extreme rainfall, which probably led the neural network to a local minimum outside of the range of the training data. Therefore, the extrapolation performed by the neural network was less accurate than interpolation (Maier and Dandy, 2000). This issue is particularly relevant in the case of the assemblage D but it almost certainly applies to all the six models to a certain degree.

4.3. Patterns of periodicity

The environmental conditions in GoT appear to be more periodic

than in GoV. This can be partly explained by the shorter length of the time series in GoV (70 months versus 150 months in GoT) and the proportion of missing data. The Moran eigenvectors eliminate missing values in the time-series at the expense of some bias in the shortest and longest frequency vectors (Brind'Amour et al., 2018). Nevertheless, the periodic components of the GoT explained additional ~6.6 % variation in environmental parameters in GoV, thus suggesting a more equal role of autocorrelation in both areas. In GoV, the N-S component of the wind is as periodic as in GoT, as Bora and southern winds alternate (Supplementary material S 6). On the contrary, the E-W component does not show periodicity in GoV, probably because of the weaker dominance of the Jugo (Scirocco) among the southern winds (Poulain et al., 2001). The strength of the thermocline is more irregular in GoV, but this may be due to both the higher number of missing values for this specific factor compared to its counterpart in GoT and the coastal and meteorological influences (Alberotanza et al., 2004). The combination of these two parameters (E.W component and thermocline strength) is responsible for the slightly lower percentage of variance explained by periodic components in GoV overall. From the analysis of variance, it appears that a relatively large portion of variance in GoV is explained by the periodic components of the environmental parameters in GoT (~26.9 %). This shared variance expresses the extent to which the two environments are similar in periodicity. Temperature and thermocline cycles ($\rho = 0.82$ and 0.57 , respectively), along with seasonal variations in wind and rivers ($\rho = 0.63$ and 0.49 , respectively), are the source of the common periodicity. As expected, the non periodic components did not share explanatory power with the periodic components of GoT and GoV, but explained another 11.0 % of the variance of GoV non periodic components. This 11.0 % of the variance represents anomalous events that occurred at the mesoscale level. Rather than trying to determine which parameters are responsible for this anomaly, it is more important to note that unexplained non-periodic events in GoV account for ~50 % of the variance. This suggests that the two LTER sites do not share the majority of non-periodic events (11.0 % shared vs 50.6 %) but the environment in the northern Adriatic is mainly uniform in its periodic part (33.5 % vs 12.1 %).

Our results also confirm the relationship between the phytoplankton community in the GoT and the periodic components of the environmental parameters, which can be mirrored to a nearby area of the northern Adriatic (GoV). This could be confirmed only when a fine structure of the phytoplankton community in GoT was taken into consideration (i.e. the fine phytoplankton assemblage partition from Vascotto et al. (2021)). Although our results suggest that phytoplankton community is more structured by the periodic components of the environment, we should be cautious to argue the opposite as well, since we could not use all the assemblages from Vascotto et al. (2021). The short-lived assemblages that were excluded from the analysis could have represented the deviations resulted from the non-periodic components of the environment.

Current dynamics, as one of these important mesoscale engineers, determine water masses with similar histories whose lifetimes fall within the range of phytoplankton blooms; i.e. few weeks (d'Ovidio et al., 2010). In northern Adriatic such currents connect the two study areas by persistent cyclonic sub-gyres (Poulain et al., 2001; Petelin et al., 2013). Moreover, this circulation path is even strengthened during Bora events (Boicourt et al., 2021). Surface waters from GoT reach the western part of the northern Adriatic, while deeper waters from GoV are transported back to the eastern part with a branch entering the GoT (Malacčić et al., 2012). This cyclonic circulation is responsible also for the occasional surface summer advection of riverine waters, nutrients and phytoplankton from the western to the eastern side of the Adriatic (Vilicic et al., 2013). Alternatively, during Scirocco events surface circulation is generally split in two branches, one entering the GoT and the other recirculating in a basin scale cyclonic gyre (Boicourt et al., 2021). The cyclonic connectivity could explain some of the features of the phytoplankton community in the northern Adriatic. In fact, two of the

assemblages occurring during windy months (assemblages E and F) presented a one-month delay in their phenology between the two sides of the basin indicating a synchronized change in water column conditions. Moreover, the first appearance of the assemblage E in September 2010, which corresponded to the long-lasting *Pseudo-nitzschia* bloom in GoT (Vascotto et al., 2021), matched one of the intrusion of Po River plume in GoT in August 2010 (Vilicic et al., 2013).

Stratification of the water column is another mesoscale characteristic that affects the phytoplankton community in northern Adriatic, acting in periodical patterns but differently in both areas. When the winter winds calm down, the stratification in the GoV moves eastward starting at the end of spring in the western part and reaching the strongest stratification condition at the end of summer (Degobbis et al., 2000). In GoT, on the contrary, the stratification reaches its maximum at the end of spring, when Soča River plume remains blocked in the surface layer of the gulf moving clockwise (Malacic and Petelin, 2009). Therefore, during stratified water column conditions in spring and summer the phytoplankton community seems to be more affected by local events, which can be seen in the temporally non-synchronized formation of assemblage B. Moreover, this assemblage disappeared after 2012 in GoT, when there was also an interruption of successive comparison of assemblage C in July. These changes were not mirrored by any change in GoV community succession, indicating that during this part of the year the two areas are less connected. Similar results were obtained in the Gulf of Naples from Ribera d'Alcalà et al. (2004) who observed that winter and autumn blooms were related to basin-wide meteorological events, whereas late spring-summer blooms were local phenomena, driven by lateral advection. It is possible, finally, that the increase in Soča River discharge (Supplementary material Fig. 5) could have affected these changes in GoT phytoplankton phenology.

The importance of seasonality for the northern Adriatic phytoplankton community has been highlighted several times in recent years (Mozetič et al., 1998; Cerino et al., 2019; Salgado-Hernanz et al., 2019). Besides confirming this importance, our work also extended the relevance of this relationship to assemblages' patterns. The succession of assemblages is linked to the seasonality of environmental forcing, both at mesoscale (Bora events) and at local scale (stratification and river discharge). Bora winds, which contribute to the cyclonic gyre connecting the basin at mesoscale, are decreasing in frequency and strength most likely due to global warming (Pirazzoli and Tomasin, 2002). On the other hand, anomalous meteorological events, such as marine heat waves, have increased in frequency in the last years (Boicourt et al., 2021) and have been forecasted to increase even more in near future (Lionello, 2012). It has been forecasted that future conditions of global temperature increase predicted by the International Panel on Climate Change (IPCC) will pose medium to high risk to the structure and phenology of Mediterranean marine ecosystems (Ali et al., 2022) our results seem to confirm this expectations. Increased stratification due to lack of winds and increased air temperature should lead, according the Magalef's succession model (Magalef, 1978), to the rise of motile and mixotrophic dinoflagellates over diatoms. Moreover, the enhanced stratification could also increase the chance of episodic outburst of phytoplankton biomass during high river discharge (Lowery, 1998; Rabalais et al., 2014). Alternatively, such water column condition could lead to a main assemblage succession sensu Reynolds (2006) from high surface/volume colonist species to biomass conserving stress-tolerant species (Reynolds, 2006). The reduction in phytoplankton size in stratified conditions should also lead to a change in trophic fluxes with an increased importance of the microbial loop pathway for zooplankton grazing (Lewandowska et al., 2014). Moreover, the reduced connectivity between the two sides could increase the sensitivity of the habitat to local events such as droughts or freshwater pulses, which are mostly non-periodic. As concerns phytoplankton community, an increasing disorder in the succession of assemblages has been observed in the GoT in recent years (Vascotto et al., 2021) possibly indicating a loss in connectivity.

The 11th Workshop of International Association of Phytoplankton Taxonomy and Ecology (IAP) proposed 10 rules for the formation of community assembly (Reynolds et al., 2000). According to these, the factors determining a particular assemblage at a particular point of time are not only those determining the realised niche, but they also depend on the precedent state of the community and stochasticity (Reynolds et al., 2000). In the present study, the physical parameters considered are those associated with the formation of realised phytoplankton niches, e.g., temperature and salinity (Irwin et al., 2012; Brun et al., 2015), stratification and river discharge (Kemp and Villareal, 2018) and we found differences in taxonomic composition under similar environmental conditions and consequently similar realised niches. The presence in our results of different indicative phytoplankton taxa inside the same niche can be explained in the light of IAP's rules. Moreover, the differences in taxonomic composition under similar conditions seem to indicate a pattern of community succession consistent with the lumpy coexistence theory (Scheffer and van Nes, 2006). Within this theory, Sakavara et al. (2018) showed that assemblage-like structures arise from resource fluctuations (Sakavara et al., 2018). In line with this recent ecological theory, the periodic components of our niche-forming environmental parameters were key in building working models for the assemblages' phenology. There is a close relationship between IAP's rules and lumpy coexistence theory that has not been pointed out so far in literature. The concepts of niche and stochasticity coexist in both frameworks and both can explain the complex patterns seen in the formation of phytoplankton assemblages in our results.

5. Conclusions

In this study, we investigated the relative importance of environmental factors and temporal periodicity in governing the structure of the phytoplankton community in the northern Adriatic. We also aimed to determine whether the influence of these factors extends to the mesoscale. The results show that there is an overlap of phenomena in the northern Adriatic, with both widespread periodic processes and local non-periodic events affecting the phytoplankton community at the basin scale. A portion of the phytoplankton assemblages have similar indicative taxa or respond similarly to the environment at the basin-wide level. Here, autocorrelation contributes to the explanatory power of environmental factors and suggests that the northern Adriatic can be treated partially as a single environment when considering periodic patterns of recurrent phytoplankton assemblages. In the context of global climate change, the connectivity of this environment and the existence and succession of phytoplankton assemblages are threatened by the reduction of wind-driven circulation and the increasing disorder of environmental conditions. Both IAP's rules for community assembly and lumpy coexistence theory explain the taxa composition in our phytoplankton assemblages drawing a connection between the two models.

Declaration of generative AI in scientific writing

During the preparation of this work the authors used InstaText (<https://instatext.io/>) to check the grammar and style. After using this tool/service, the authors reviewed and edited the content as needed and take full responsibility for the content of the publication.

CRedit authorship contribution statement

Ivano Vascotto: Conceptualization, Formal analysis, Methodology, Writing – original draft, Writing – review & editing, Visualization. **Fabrizio Bernardi Aubry:** Supervision, Writing – review & editing. **Mauro Bastianini:** Data curation, Writing – review & editing. **Patricija Mozetič:** Supervision, Writing – review & editing. **Stefania Finotto:** Resources. **Janja Francé:** Conceptualization, Supervision, Writing – review & editing.

Declaration of competing interest

The authors declare that they have no known competing financial interests or personal relationships that could have appeared to influence the work reported in this paper.

Data availability

The raw environmental data from the GoT can be found at the following links; for the oceanographic data: <https://www.nib.si/mbp/en/oceanographic-data-and-measurements/buoy-2/new-scalar-plots>, for the river discharge data: <https://www.arso.gov.si/en/water/data/>, and for the meteorological data: <https://meteo.arso.gov.si/met/sl/archive/>.

The raw phytoplankton data and the environmental parameters from GoV are stored in the Marine Data Archive (MDA) <https://marinedataarchive.org/> following the public directory path: ASSEMBLE Plus - Public/TA Data/North Adriatic Phytoplankton Assemblages/.

The assemblage's probability and Indicative Index results are stored in the Marine Data Archive (MDA) and are findable at IMIS record <https://www.vliz.be/en/imis?module=dataset&dasid=8110>.

The R code for the Moran's eigenvector decomposition and RDA as well as the Python code for the neural network construction and training can be found in the public repository GitHub at the following link: <https://github.com/ivanovascotto/NorthAdriaticPhytoplanktonAssemblages>.

Acknowledgements

The research leading to these results received funding from the European Union's Horizon 2020 research and innovation programme under grant agreement No 730984, ASSEMBLE Plus project and by Slovenian Research Agency (ARIS), grant number P1-0237.

The GoT and the GoV are included in the Italian (LTER-Italy) and Slovenian (LTER-Slovenia), European (LTER-Europe) and International (LTER-International) Long-Term Ecological Research (LTER)

networks: the time series analysed in this paper was gathered in the context of these networks. Phytoplankton data of the Slovenian LTER originates from the national monitoring program financed by the Slovenian Environment Agency of the Ministry of Environment and Spatial Planning.

Authors wish to thank Milijan Šiško for phytoplankton species identification and enumeration, the crew of R/V Sagita for the field work and curators of oceanographic buoy Vida for data generation.

Appendix A. Supplementary data

Supplementary data to this article can be found online at <https://doi.org/10.1016/j.scitotenv.2023.169814>.

References

- Abadi, M., A. Agarwal, P. Barham, E. Brevdo, Z. Chen, C. Citro, G. S. Corrado, A. Davis, J. Dean, M. Devin, S. Ghemawat, I. Goodfellow, A. Harp, G. Irving, M. Isard, R. Jozefowicz, Y. Jia, L. Kaiser, M. Kudlur, J. Levenberg, D. Mané, M. Schuster, R. Monga, S. Moore, D. Murray, C. Olah, J. Shlens, B. Steiner, I. Sutskever, K. Talwar, P. Tucker, V. Vanhoucke, V. Vasudevan, F. Viégas, O. Vinyals, P. Warden, M. Wattenberg, M. Wicke, Y. Yu and X. Zheng (2015). "TensorFlow: Large-scale machine learning on heterogeneous systems."
- Alberotanza, L., Chiggiato, J., Profeti, G., 2004. Analysis of the seasonal stratification at the Acqua Alta oceanographic tower, northern Adriatic Sea. *Int. J. Remote Sens.* 25 (7–8), 1473–1480.
- Ali, E., Cramer, W., Carnicer, J., Georgopoulou, E., Hilmi, N.J.M., Le Cozannet, G., Lionello, P., 2022. Cross-chapter paper 4: Mediterranean region. *Climate change 2022: Impacts, adaptation and vulnerability*. In: Pörtner, H.O., Roberts, D.W., Tignor, M., et al. (Eds.), Contribution of Working Group II to the Sixth Assessment Report of the Intergovernmental Panel on Climate Change. Cambridge University Press, Cambridge, UK and New York, NY, USA, pp. 2233–2272.
- Ayata, S.-D., Irissou, J.-O., Aubert, A., Berline, L., Dutay, J.-C., Mayot, N., Nieblas, A.-E., D'Ortenzio, F., Palmieri, J., Reygondeau, G., Rossi, V., Guieu, C., 2018. Regionalisation of the Mediterranean basin, a MERMEEX synthesis. *Prog. Oceanogr.* 163, 7–20.
- Bernardi Aubry, F., Cossarini, G., Aciri, F., Bastianini, M., Bianchi, F., Camatti, E., De Lazzari, A., Pugnelli, A., Solidoro, C., Socal, G., 2012. Plankton communities in the northern Adriatic Sea: patterns and changes over the last 30 years. *Estuar. Coast. Shelf Sci.* 115, 125–137.
- Blasius, B., Huppert, A., Stone, L., 1999. Complex dynamics and phase synchronization in spatially extended ecological systems. *Nature* 27, 354–359.
- Boicourt, W.C., Ličer, M., Li, M., Vodopivec, M., Malačić, V., 2021. Sea State: Recent Progress in the Context of Climate Change. *Coastal Ecosystems in Transition: A Comparative Analysis of the Northern Adriatic and Chesapeake Bay*. John Wiley & Sons, Malone C. Thomas, A. Malej and J. Faganeli.
- Brind'Amour, A., Mahévas, S., Legendre, P., Bellanger, L., 2018. Application of Moran eigenvector maps (MEM) to irregular sampling designs. *Spatial Statistics* 26, 56–68.
- Brun, P., Vogt, M., Payne, M.R., Gruber, N., O'Brien, C.J., Buitenhuis, E.T., Le Quéré, C., Leblanc, K., Luo, Y.-W., 2015. Ecological niches of open ocean phytoplankton taxa. *Limnol. Oceanogr.* 60 (3), 1020–1038.
- Brush, M.J., Mozetič, P., Francé, J., Aubry, F.B., Djakovac, T., Faganeli, J., Harris, L.A., Niesen, M., 2021. Phytoplankton Dynamics in a Changing Environment. John Wiley & Sons.
- Cabrini, M., Fornasaro, D., Cossarini, G., Lipizer, M., Virgilio, D., 2012. Phytoplankton temporal changes in a coastal northern Adriatic site during the last 25 years. *Estuar. Coast. Shelf Sci.* 115, 113–124.
- Cerino, F., Fornasaro, D., Kralj, M., Giani, M., Cabrini, M., 2019. Phytoplankton temporal dynamics in the coastal waters of the North-Eastern Adriatic Sea (Mediterranean Sea) from 2010 to 2017. *Nature Conserv.* 34, 343–372.
- Cibic, T., Comici, C., Bussani, A., Del Negro, P., 2012. Benthic diatom response to changing environmental conditions. *Estuar. Coast. Shelf Sci.* 115, 158–169.
- Cloern, J.E., Jassby, A.D., 2010. Patterns and scales of phytoplankton variability in estuarine-coastal ecosystem. *Estuar. Coasts* 33, 230–241.
- Cozzi, S., Giani, M., 2011. River water and nutrient discharges in the northern Adriatic Sea: current importance and long term changes. *Cont. Shelf Res.* 31 (18), 1881–1893.
- Degobbi, D., Precali, R., Ivancic, I., Smoldaka, N., Fuks, D., Kveder, S., 2000. Long-term changes in the northern Adriatic ecosystem related to anthropogenic eutrophication. *Int. J. Environ. Pollut.* 13 (1–6), 495–533.
- d'Ovidio, F., De Monte, S., Alvain, S., Dandonneau, Y., Levy, M., 2010. Fluid dynamical niches of phytoplankton types. *Proc. Natl. Acad. Sci. U. S. A.* 107 (43), 18366–18370.
- Dray, S., G. Blanchet, D. Borcard, G. Guenard, T. Jombart, G. Larocque, P. Legendre, N. Madi and H. H. Wagner (2016). "adespatial: Multivariate Multiscale Spatial Analysis. R package version 0.0-7."
- Dufrene, M., Legendre, P., 1997. Species assemblages and Indicator species: the need for a flexible asymmetrical approach. *Ecol. Monogr.* 67 (3), 345.
- Francé, J., Varkitzi, I., Stanca, E., Cozzoli, F., Skejčić, S., Ungaro, N., Vascotto, I., Mozetič, P., Ninčević Gladan, Ž., Assimakopoulou, G., Pavlidou, A., Zervoudaki, S., Pagou, K., Bassett, A., 2021. Large-scale testing of phytoplankton diversity indices for environmental assessment in Mediterranean sub-regions (Adriatic, Ionian and Aegean seas). *Ecol. Indic.* 126, 107630.
- Gačić, M., Lascaratos, A., Manca, B.B., Mantziafou, A., 2001. Adriatic deep water and interaction with the eastern mediterranean sea. *Physical oceanography of the Adriatic Sea: past present future*. B. Cushman-Roisin, M. Gačić, P.-M. Poulain and A. Artegiani, Kluwer Academic Publishers. 6, 111–142.
- Godrić, J., Marić, D., Tomazić, I., Precali, R., Pfannkuchen, M., 2013. Seasonal phytoplankton dynamics in the coastal waters of the North-Eastern Adriatic Sea. *J. Sea Res.* 77, 32–44.
- Harding, L., 1994. Long-term trends in the distribution of phytoplankton in Chesapeake Bay: roles of light, nutrients and streamflow. *Mar. Ecol. Prog. Ser.* 104, 267–291.
- Hubbel, S.P., 2005. The neutral theory of biodiversity and biogeography and Stephen Jay Gould. *Paleobiology* 31 (2), 122–132.
- Hutchinson, G.E., 1941. Ecological aspects of succession in natural populations. *Am. Nat.* 75 (760), 406–418.
- Irwin, A.J., Nelles, A.M., Finkel, Z.V., 2012. Phytoplankton niches estimated from field data. *Limnol. Oceanogr.* 57 (3), 787–797.
- Jeffries, M.A., Lee, C.M., 2007. A climatology of the northern Adriatic Sea's response to bora and river forcing. *J. Geophys. Res.* 112.
- Jenkins, D.G., Ricklefs, R.E., 2011. Biogeography and ecology: two views of one world. *Philos. Trans. R. Soc. Lond. Ser. B Biol. Sci.* 366 (1576), 2331–2335.
- Kemp, A.E.S., Villareal, T.A., 2018. The case of the diatoms and the muddled mandalas: time to recognize diatom adaptations to stratified waters. *Prog. Oceanogr.* 167, 138–149.
- Legendre, P., Legendre, L., 2012. Numerical ecology. Elsevier.
- Levy, M., Jahn, O., Dutkiewicz, S., Follows, M.J., d'Ovidio, F., 2015. The dynamical landscape of marine phytoplankton diversity. *J. R. Soc. Interface* 12 (111), 20150481.
- Levy, M., Franks, P.J.S., Smith, K.S., 2018. The role of submesoscale currents in structuring marine ecosystems. *Nat. Commun.* 9 (1), 4758.
- Lewandowska, A.M., Boyce, D.G., Hofmann, M., Matthiessen, B., Sommer, U., Worm, B., 2014. Effects of sea surface warming on marine plankton. *Ecol. Lett.* 17 (5), 614–623.
- Lionello, P., 2012. The climate of the venetian and north Adriatic region: variability, trends and future change. *Phys. Chem. Earth* 40-41 (1–8).

- Lowery, T.A., 1998. Modelling estuarine eutrophication in the context of hypoxia, nitrogen loadings, stratification and nutrient ratios. *J. Environ. Manag.* 52 (3), 289–305.
- Maier, H.R., Dandy, G.C., 2000. Neural networks for the prediction and forecasting of water resources variables: a review of modelling issues and applications. *Environ. Model. Softw.* 15, 101–124.
- Malačić, V., Petelin, B., 2001. In: Cushman-Roisin, B., Gačić, M., Poulain, P.-M., A. (Eds.), *Regional Studies. Physical Oceanography of the Adriatic Sea: Past, Present, and Future*. Artegianni, Kluwer Academic Publishers, pp. 167–181.
- Malačić, V., Petelin, B., 2009. Climatic circulation in the Gulf of Trieste (northern Adriatic). *J. Geophys. Res. Oceans* 114 (C7).
- Malačić, V., Celio, M., Cermelj, B., Bussani, A., Comici, C., 2006. Interannual evolution of seasonal thermohaline properties in the Gulf of Trieste (northern Adriatic) 1991–2003. *J. Geophys. Res.* 111 (C8).
- Malačić, V., Petelin, B., Vodopivec, M., 2012. Topographic control of wind-driven circulation in the northern Adriatic. *J. Geophys. Res. Oceans* 117 (C6).
- Malej, A., Mozetič, P., Malačić, V., Turk, V., 1997. Response of summer phytoplankton to episodic meteorological events (gulf of Trieste, Adriatic Sea). *Mar. Ecol.* 18 (3), 273–288.
- Margalef, R., 1978. Life-forms of phytoplankton as survival alternatives in an unstable environment. *Oceanol. Acta* 1 (4), 493–509.
- Marić Pfannkuchen, D., Godrijan, J., Smolaka Tanković, M., Baričević, A., Kužat, N., Djakovac, T., Pustijanac, E., Jahn, R., Pfannkuchen, M., 2018. The ecology of one cosmopolitan, one newly introduced and one occasionally advected species from the genus *Skeletonema* in a highly structured ecosystem, the northern Adriatic. *Microb. Ecol.* 75, 674–687.
- Marić, D., Kraus, R., Godrijan, J., Supić, N., Djakovac, T., Precali, R., 2012. Phytoplankton response to climatic and anthropogenic influences in the north-eastern Adriatic during the last four decades. *Estuar. Coast. Shelf Sci.* 115, 98–112.
- Martin, A.P., 2003. Phytoplankton patchiness: the role of lateral stirring and mixing. *Prog. Oceanogr.* 57 (2), 125–174.
- May, R., 1976. Simple mathematical models with very complicated dynamics. *Nature* 261 (459–467).
- Mozetič, P., Fonda Umani, S., Cataletto, B., Malej, A., 1998. Seasonal and inter-annual plankton variability in the Gulf of Trieste (northern Adriatic). *J. Mar. Sci.* 55 (711–722).
- Mozetič, P., Francé, J., Kogovšek, T., Talaber, I., Malej, A., 2012. Plankton trends and community changes in a coastal sea (northern Adriatic): bottom-up vs. top-down control in relation to environmental drivers. *Estuar. Coast. Shelf Sci.* 115, 138–148.
- Neri, F., Romagnoli, T., Accoroni, S., Campanelli, A., Marini, M., Grilli, F., Totti, C., 2022. Phytoplankton and environmental drivers at a long-term offshore station in the northern Adriatic Sea (1988–2018). *Cont. Shelf Res.* 242, 104746.
- Oksanen, J., Blanchet, F.G., Kindt, R., Legendre, P., Minchin, P.R., O'hara, R.B., Simpson, G.L., Solymos, P., Stevens, M.H.H., Wagner, H., Oksanen, M.J., 2013. Package 'vegan. Community ecology package, version 2 (9), 1–295.
- Orlanski, I., 1975. A rational subdivision of scales for atmospheric processes. *Bull. Am. Meteorol. Soc.* 56 (5), 527–530.
- Petelin, B., Kononenko, I., Malačić, V., Kukar, M., 2013. Multi-level association rules and directed graphs for spatial data analysis. *Expert Syst. Appl.* 40 (12), 4957–4970.
- Pirazzoli, P.A., Tomasin, A., 2002. Recent evolution of surge-related events in the northern Adriatic area. *J. Coast. Res.* 537–554.
- Platt, T., Denmann, K.L., 1975. Spectral analysis in ecology. *Annu. Rev. Ecol. Syst.* 6, 189–210.
- Poulain, P.-M., Kourafalou, V.H., Cushman-Roisin, B., 2001. In: Cushman-Roisin, B., Gačić, M., Poulain, P.-M., A. (Eds.), *Northern Adriatic Sea. Physical Oceanography of the Adriatic Sea: Past, Present, and Future*. Artegianni, Kluwer Academic Publishers, pp. 167–181.
- Ptacnik, R., Solimini, A.G., Andersen, T., Tamminen, T., Brettum, P., Lepistö, L., Willén, E., Rekolainen, S., 2008. Diversity predicts stability and resource use efficiency in natural phytoplankton communities. *Proc. Nat. Acad. Sci. U.S.A.* 105 (13), 5134–5138.
- Rabalais, N.N., Cai, W.-J., Carstensen, J., Conley, D.J., Fry, B., Hu, X., Quinones-Rivera, Z., Rosenberg, R., Slomp, C.P., Turner, R.E., 2014. Eutrophication-driven deoxygenation in the coastal ocean. *Oceanography* 27 (1), 172–183.
- Reynolds, C., 1980. Phytoplankton assemblages and their periodicity in stratifying Lake systems. *Holarctic Ecol.* 3 (3), 141–159.
- Reynolds, C.S., 2006. *The Ecology of Phytoplankton*. Cambridge University Press.
- Reynolds, C., Dokulil, M., Padišak, J., 2000. Understanding the assembly of phytoplankton in relation to the trophic spectrum: where are we now? *Hydrobiologia* 424, 147–152.
- Ribera d'Alcalá, M., Conversano, F., Corato, F., Licandro, P., Mangoni, O., Marino, D., Mazzocchi, M.G., Modigh, M., Montresor, M., Nardella, M., Saggiomo, V., Sarno, D., Zingone, A., 2004. Seasonal patterns in plankton communities in a pluriannual time series at a coastal Mediterranean site (gulf of Naples): an attempt to discern recurrences and trends. *Sci. Mar.* 68 (1), 65–83.
- Ricklefs, R.E., Jenkins, D.G., 2011. Biogeography and ecology: towards the integration of two disciplines. *Philos. Trans. R. Soc. Lond. Ser. B Biol. Sci.* 366 (1576), 2438–2448.
- Roelke, D.L., Spatharis, S., 2015a. Phytoplankton assemblage characteristics in recurrently fluctuating environments. *PLoS One* 10 (3), e0120673.
- Roelke, D.L., Spatharis, S., 2015b. Phytoplankton succession in recurrently fluctuating environments. *PLoS One* 10 (3), e0121392.
- Sakavara, A., Tsiartsis, G., Roelke, D.L., Mancy, R., Spatharis, S., 2018. Lumpy species coexistence arises robustly in fluctuating resource environments. *PNAS* 115 (4), 738–743.
- Salgado-Hernanz, P.M., Racault, M.F., Font-Muñoz, J.S., Basterretxea, G., 2019. Trends in phytoplankton phenology in the Mediterranean Sea based on ocean-colour remote sensing. *Remote Sens. Environ.* 221, 50–64.
- Scheffer, M., van Nes, E.H., 2006. Self-organized similarity, the evolutionary emergence of groups of similar species. *Proc. Natl. Acad. Sci. U. S. A.* 103 (16), 6230–6235.
- Soininen, J., 2010. Species turnover along abiotic and biotic gradients: patterns in space equal patterns in time? *BioScience* 60 (6), 433–439.
- Stone, L., 1993. Period-doubling reversals and chaos in simple ecological models. *Nature* 365, 617–620.
- Talaber, I., Francé, J., Mozetič, P., 2014. How phytoplankton physiology and community structure adjust to physical forcing in a coastal ecosystem (northern Adriatic Sea). *Phycologia* 53 (1), 74–85.
- Tobler, W.R., 1970. A computer movie simulating urban growth in the Detroit region. *Econ. Geogr.* 46, 234–240.
- Totti, C., Romagnoli, T., Accoroni, S., Coluccelli, A., Pellegrini, M., Campanelli, A., Grilli, F., Marini, M., 2019. Phytoplankton communities in the northwestern Adriatic Sea: Interdecadal variability over a 30-years period (1988–2016) and relationships with meteorological drivers. *J. Mar. Syst.* 193, 137–153.
- Turk Dermastia, T., Cerino, F., Stankovic, D., France, J., Ramsak, A., Znidaric Tusek, M., Beran, A., Natali, V., Cabrini, M., Mozetič, P., 2020. Ecological time series and integrative taxonomy unveil seasonality and diversity of the toxic diatom *pseudo-nitzschia* H. Peragallo in the northern Adriatic Sea. *Harmful Algae* 93, 101773.
- Vallina, S.M., Follows, M.J., Dutkiewicz, S., Montoya, J.M., Cermeño, P., Loreau, M., 2014. Global relationship between phytoplankton diversity and productivity in the ocean. *Nat. Commun.* 5, 4299.
- Vascotto, I., Mozetič, P., Francé, J., 2021. Phytoplankton time-series in a LTER site of the Adriatic Sea: methodological approach to decipher community structure and indicative taxa. *Water* 13 (15), 2045.
- Vilicic, D., Kuzmic, M., Tomazič, I., Ljubešić, Z., Bosak, S., Precali, R., Djakovac, T., Marić, D., Godrijan, J., 2013. Northern Adriatic phytoplankton response to short Po River discharge pulses during summer stratified conditions. *Mar. Ecol.* 34 (4), 451–466.
- Winder, M., Cloern, J.E., 2010. The annual cycles of phytoplankton biomass. *Philosophical Transaction of The Royal Society* 365, 3215–3226.
- Zhang, Q., Cozzi, S., Palinkas, C., Giani, M., 2020. Recent status and long-term trends in freshwater discharge and nutrient inputs. *Coastal Ecosystems in Transition: A Comparative Analysis of the Northern Adriatic and Chesapeake Bay* 7–19.